Ecological Informatics 82 (2024) 102708

Contents lists available at ScienceDirect

Ecological Informatics

journal homepage: www.elsevier.com/locate/ecolinf

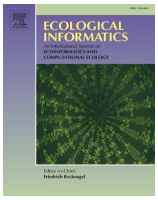

Drone imagery and deep learning for mapping the density of wild Pacific oysters to manage their expansion into protected areas

Aser Mata [a,*], David Moffat [a], Sílvia Almeida [b], Marko Radeta [b,c,d], William Jay [a], Nigel Mortimer [e], Katie Awty-Carroll [f,1], Oliver R. Thomas [a,g], Vanda Brotas [h], Steve Groom [a]

[a] Plymouth Marine Laboratory, Prospect Place, Plymouth PL1 3DH, UK
[b] Marine and Environmental Sciences Centre (MARE), Aquatic Research Network (ARNET), Regional Agency for the Development of Research, Technology and Innovation (ARDITI), Funchal 9020-105, Portugal
[c] Wave Labs, Faculty of Exact Sciences and Engineering, University of Madeira, Funchal 9020-105, Portugal
[d] Department of Astronomy, Faculty of Mathematics, University of Belgrade, Belgrade 11000, Serbia
[e] South Devon Area of Outstanding Natural Beauty, Follaton House, Plymouth Road, Totnes TQ9 5NE, UK
[f] The Alan Turing Institute, British Library, 96 Euston Road, London NW1 2DB, UK
[g] Plymouth University, Drake Circus, Plymouth PL4 8AA, UK
[h] Marine and Environmental Sciences Centre (MARE), Lisbon University, Lisbon, Campo Grande 016, Portugal

ARTICLE INFO

Keywords:
Pacific oysters
Invasive species
Convolutional neural networks
Deep learning
Drone
Remote sensing
Ecological management

ABSTRACT

The recent expansion of wild Pacific oysters already had negative repercussions on sites in Europe and has raised further concerns over their potential harmful impact on the balance of biomes within protected areas. Monitoring their colonisation, especially at early stages, has become an urgent ecological issue. Current efforts to monitor wild Pacific oysters rely on "walk-over" surveys that are highly laborious and often limited to specific areas of easy access. Remotely Piloted Aircraft Systems (RPAS), commonly known as drones, can provide an effective tool for surveying complex terrains and detect Pacific oysters. This study provides a novel workflow for automated detection, counting and mapping of individual Pacific oysters to estimate their density per square meter by using Convolutional Neural Networks (CNNs) applied to drone imagery. Drone photos were collected at low tides and altitudes of approximately 10 m across a variety of cases of rocky shore and mudflats scenarios. Using object detection, we compared how different Convolutional Neural Networks (CNNs) architectures including YOLOv5s, YOLOv5m, TPH-YOLOv5 and FR-CNN performed in the detection of Pacific oysters over the surveyed areas. We report the precision of our model at 88% with a difference in performance of 1% across the two sites. The workflow presented in this work proposes the use of grid maps to visualize the density of Pacific oysters per square meter towards ecological management and the creation of time series to identify trends.

1. Introduction

The *Crassotrea gigas* (or *Magallana gigas*), commonly known as the Pacific oyster, is a species indigenous to the Northwest Pacific coast. Due to their commercial value, Pacific oysters were introduced across 73 countries worldwide mainly in America, Europe and Africa (Ruesink et al., 2005). In the United Kingdom, Pacific oysters are well documented as a non-native invasive species (Walne and Helm, 1979), first introduced into the River Blackwater (Essex, UK) in 1926 for aquaculture (Utting and Spencer, 1992). Since 2017, wild Pacific oysters has been reported in large numbers on coastal and estuarine areas across the Southwest of England (Natural England, 2021). The impact of the dissemination of wild Pacific oysters across Europe has become a growing concern in recent years (Herbert et al., 2016). Furthermore, as a result of climate change, their numbers are expected to keep increasing due to the warmer climates in Europe (King et al., 2020; Rinde et al., 2017; Wilson et al., 2024).

Pacific oysters have a high reproduction rate and their colonisation can induce the development of biogenic reefs. Biogenic reefs can introduce diversities, services and food items based on a non-native ecology as well as inhibit or block the access to the sediments that could otherwise be used as foraging habitat for other species, displacing

* Corresponding author.
E-mail address: asm@pml.ac.uk (A. Mata).
[1] Work carried out while at Plymouth Marine Laboratory.

https://doi.org/10.1016/j.ecoinf.2024.102708
Received 21 February 2024; Received in revised form 28 June 2024; Accepted 28 June 2024
Available online 8 July 2024

and or changing the original community structure (Green and Crowe, 2014). Therefore, the unmanaged dissemination of Pacific oysters can lead to a reduction in the number of prey for different species of birds and fish, altering the balance of biotopes and precipitating the loss of original species in intertidal areas. This effect can have a significant negative impact, especially within Marine Protected Areas (MPAs).

The *Saccostrea* and *Crassotrea* oysters are predominantly located in intertidal regions and the Pacific oysters or *Crassotrea gigas* are no exception (Herbert et al., 2012). On the other hand, the *Ostrea* to which the UK native oyster *Ostrea edulis* form part of, are mainly found in subtidal areas and display a different shape and colour (Perry et al., 2023).

The recent expansion of Pacific oysters into MPAs in the UK caused that several sites across Cornwall and Devon being flagged as in "unfavourable condition" (Natural England, 2021). Hence, there is a need for continuous monitoring to detect and manage the advance of Pacific oysters, ideally at early stages of colonisation. Fig. 1 shows an example of two different cases of very high density or low density of Pacific oysters. To prevent the possible negative impact of Pacific oysters in protected areas, the focus should be in the detection and number estimation in low and medium density sites (Figure as shown in 1a) before an oyster reef is created and clusters are formed (Fig. 1b). Therefore, it is important to assess the expansion of the Pacific oysters into protected areas by quantifying their individual number to plan remedial action if necessary before a tipping point is reached and large aggregates are formed (Hansen et al., 2023; Reise et al., 2006). Current detection methods in the UK include the training of volunteers to organise counting or culling surveys to eradicate them by mechanical means e.g., using chisel hammers in rocky shores (Natural England, 2021). This translates into a high manpower cost to survey regional areas.

Moreover, different intertidal regions are of difficult or impossible access to traditional on-foot surveys and thus may present a high risk to the involved personnel (e.g. mudflats or vertical cliffs). In these cases, and only when practicable, expertly trained personnel might access some of those areas and need to wear suitable equipment like mudflat walkers. This provides further challenges to survey large areas, increasing significantly the labour and costs (Jaud et al., 2019).

Remotely Piloted Aircraft Systems (RPAS), popularly known as drones, have the potential to provide a cost-effective monitoring solution for the Pacific oysters (White et al., 2022). Aerial drones not only can reduce the costs of surveys but also provide tools to monitor areas that are otherwise dangerous to access. Analysing the drone imagery to detect the Pacific oysters would allow to assess the expansion of Pacific oysters at early stages and detect hotspots providing the necessary data to act in order to mitigate their possible negative impact.

As Pacific oysters are found in intertidal areas, drone aerial surveys can be undertaken around low tides to detect them while they are exposed, avoiding as well artifacts due to turbidity or sunglint. On the other hand, Autonomous Marine Vessels (AMVs) could also be beneficial for detecting other subtidal species of oysters but AMVs are not able to operate in very shallow waters or too close to the shoreline, which makes them difficult to be deployed in intertidal regions for surveying Pacific oysters especially.

Likewise, Deep Learning (DL) can aid in the automated detection of Pacific oysters present in large amounts of drone images, which would otherwise require extensive human work (Radeta et al., 2022). Indeed, Kakehi et al. (2021) proposed the application of object detection techniques to microscopic images for identifying and counting Pacific oysters larvae collected from Matsushima and Sendai bays in Miyagi Prefecture, Japan. In this work, we applied object detection protocols and techniques similar to those employed for the detection of intertidal marine litter in drone images (Andriolo et al., 2020, 2022; Takaya et al., 2022).

In order to correctly identify Pacific oysters from different backgrounds that include rocky shores with pebbles of similar colour to the oysters, their shape must also be captured in the images. Therefore, when planning the drone survey, a Ground Sampling Distance (GSD) that makes possible to collect images of Pacific oysters with enough resolution to perform at least medium size object detection (50–300 pixels) is required (Gong et al., 2022). The GSD of a camera mounted on a drone is determined by its focal length, the number of pixels and the distance of flight altitude to the target (Andriolo et al., 2023). Adult Pacific oysters have typical lengths of 8–15 cm and can reach lengths up 20 cm, sometimes even larger. Their width present an approximate ratio 2:3 to their length. If we consider the smallest size of an adult Pacific oysters to be 8 cm long and 5 cm wide, then at least a GSD of 0.8 cm/px is required to capture the oyster with at least 50 pixels.

Other researchers (Ridge et al., 2020) published results from applying Masked R-CNN and segmentation to aerial images collected at 100 m altitudes with reported Ground Sampling Distance (GSD) of 2.2 px/cm to delineate and map the area of oyster reefs rather than detecting individual Pacific oysters. Additionally, Sadrfaridpour et al. (2021) showed how Masked R-CNN could be used to detect subtidal (non-

(a) Sparse Pacific oyster population (b) Very dense Pacific oyster population

Fig. 1. Examples of sparse and very high density of Pacific oysters in the field.

Pacific) oysters from images collected with AMVs at a distance of 3 ft (approximately 92 cm) from the seabed. As Sadrfaridpour et al. (2021) data was collected using a GoPro Hero7 Black camera, they used a GSD better than 0.06 cm/px (Wierzbicki, 2018). This means that an oyster of 8 × 5 cm will be captured in 666 pixels, therefore falling in the category of big object detection (> 300 pixels), (Gong et al., 2022). However, undertaking a drone survey in the field to cover medium to large size areas at altitudes of 1 m would not be feasible due to the amount of hours required. Hence, when planning the survey, the resolutions and sensor altitudes needed for big object detection are only recommended for very small areas and are not applicable to characterise the expansion of wild Pacific oysters. Similarly, Lin et al. (2022) used similar pixel resolutions of large object detection and reported success in modelling partially captured submerged non-Pacific oysters by applying Generative Adversarial Networks (GANs).

To the best of authors' knowledge, no case of study has been published to date that outlines the workflow to identify and count individual Pacific oysters per square meter using aerial drones for the potential deployment towards large-scale monitoring of an area of study.

Our study presents four core differences from other publications: (i) we focus on detailed and individual Pacific oyster counts using object detection; (ii) we focus on the detection of wild Pacific oysters in intertidal mudflats and rocky shores; (iii) we collected data using aerial drones flown at low altitudes and during low tides resulting in sub-centimeter pixel size that allows for identification of individual Pacific oysters as medium size objects; and (iv) we benchmark other state of the art DL architectures. Additionally, following the best practices suggested by Gonçalves et al. (2022) detecting marine litter in the intertidal region, our workflow includes the creation of grid orthomaps for best visualization of the Pacific oysters detected per square meter of the surveyed area. Using this approach, areas of higher densities of Pacific oysters can easily be identified in the map. Moreover, this makes possible to visualize on a map changes due to seasonal effects by undertaking periodic drone surveys in the same area for continuous monitoring.

2. Methodology

2.1. Study sites

A field campaign was carried out at two distinctive intertidal cases at Kingsbridge Estuary, UK (Fig. 2). Drone images were collected around low tide on each site of the estuary selected by the high number of Pacific oysters reported and their very different characteristic landscapes of mudflats and rocky shore. The two sites included in this work are:

- **Site A: Collapit Creek mudflats**. An area of approximately 1.67 ha intertidal mudflat was surveyed on 13th May 2022 shown on Fig. 3 (lat, lon = 50.259245, −3.771041).
- **Site B: Scoble Point rocky shore**. The intertidal region that follows the shoreline for approximately 250 m was surveyed on 16th May 2022, Fig. 4 (50.240164, −3.755421).

Collapit Creek (Site A) is a mudflat area of special interest for seagrass where Pacific oyster have previously been reported in exceptionally high numbers (Natural England, 2021). Moreover, this area is not accessible by boat and is very difficult to access by foot as the mud column can reach more than 1.5 m depth. Contrarily, Scoble Point (Site B) is an intertidal rocky shore with a steep coastline accessible by boat that presents a very high density of seaweed and where the Pacific oysters grow over the rocks and fill gaps.

At the Collapit Creek mudflat (Site A), drone images were collected using a DJI Phantom4 Pro v2.0 in a pre-planned grid mission using the "DJI GS Pro" mission planner software. Photos were acquired at 10 m altitude (resulting in a pixel size of ~0.3 px/cm) with a front overlap ratio of 80% and a side overlap of 70%. The camera was positioned at a

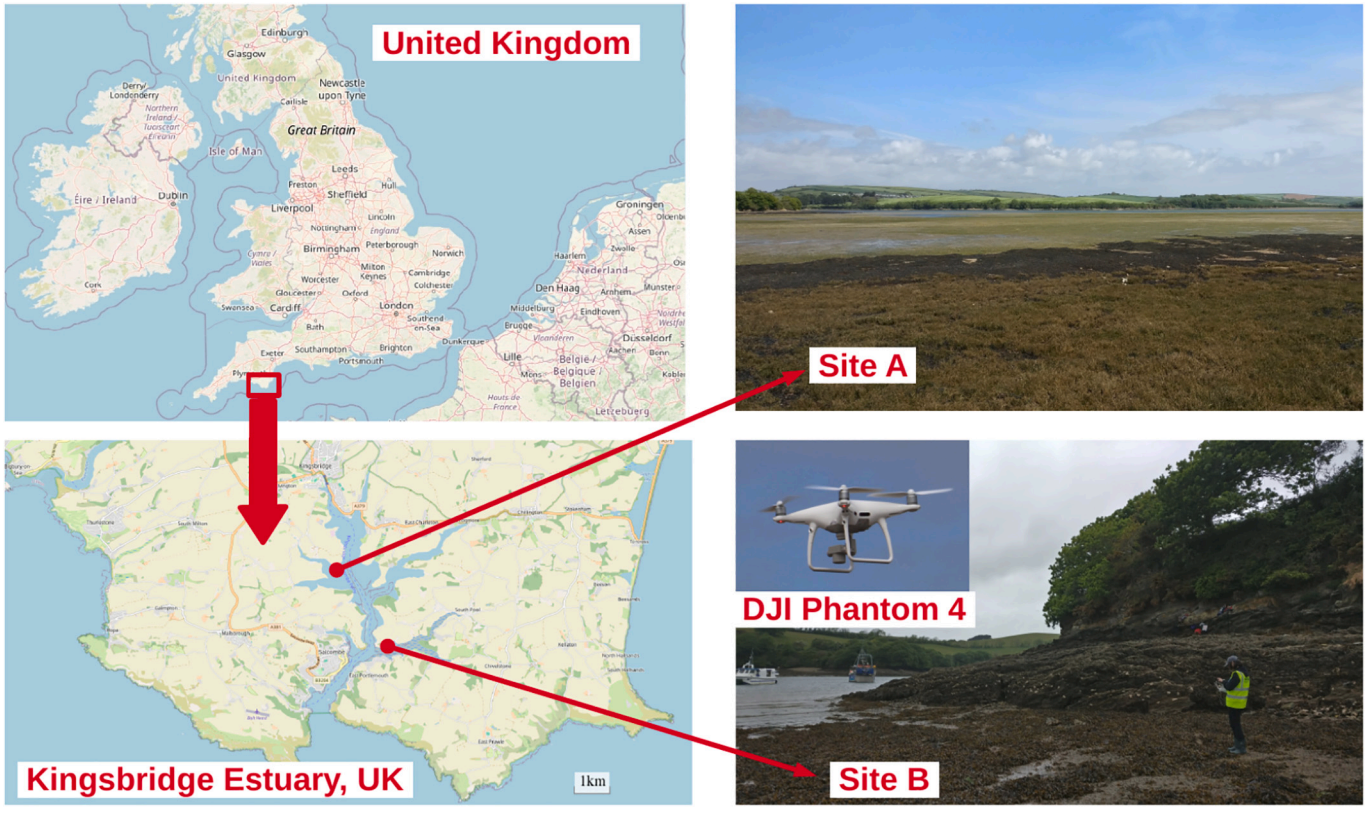

Fig. 2. The two study sites selected for this study and located in the Kingsbridge Estuary (UK). Drone surveys were carried out during low tides using a DJI Phantom 4.

Fig. 3. Drone orthomosaic of Site A, Collapit Creek mudflat (50.259245, −3.771041) collected on 13th May 2022 overlaid on a Google map image.

Fig. 4. Drone orthomosaic of Site B, Scoble Point rocky shore (50.240164, −3.755421) collected on 16th May 2022 overlaid on a Google map image.

15° angle off-nadir to minimise sun-glint effects (Schneider-Zapp et al., 2019). A total of 1964 individual drone images were collected over the mudflat during approximately 80 minutes using 4 sets of batteries.

The rocky shore (Site B) comprises a smaller site and presents a more complicated orography due to the steepness of the rocky shoreline and different obstacles such as trees. Drone images were collected with the same aircraft (DJI P4v2) and same overlapping ratios and off-nadir camera angle but at a slightly higher altitude of 12 m for most of the

site (~0.4 px/cm). Additional overlapping photos were collected by manually operating the drone at the altitudes of 9 m and 3 m to capture high densities areas in higher detail where the steepness of the terrain would have prevented the collection of images with the planned overlap. A total of 829 drone images were collected for this site using 2 sets of batteries in 40 minutes.

2.2. Data pre-processing and data annotation

Drone photos were processed using the photogrammetric technique Structure from Motion via the commercial package "Agisoft Metashape Professional" (software version 1.7.6). This software is able to identify Tie Points in the overlapping regions of the images to stitch the photos together and model the elevation of the surveyed area. A Digital Elevation Model (DEM) and orthomap were created for each site, as can be seen in Fig. 3 and Fig. 4. These orthomaps allowed for individual orthorectified images from both sites and were made freely available to other researchers (Mata, 2024). These two environments present different challenges to the DL model, particularly to ensure that rocks are not confused with Pacific oysters. The selected sites are representative of a large variety of naturally occurring intertidal landscapes (Diederich, 2006) and were selected to ensure that DL models generalize across different geographic locations.

In order to create the Pacific oyster dataset, specific subsets of each region were manually selected to make sure all different terrain types found at each site were captured: mud, rocks, and sand. These regions included areas of both sparse and dense Pacific oysters population on each sites. The images in each region contained oysters that were clearly visible and oysters partially covered with seaweed in all possible background configurations.

Individual orthorectified images covering the training and validations areas within both sizes were visually inspected to identify individual Pacific oysters. Bounding boxes were drawn for each Pacific oyster to build the tagged dataset using the Python "LabelImg" library (Tzutalin, 2015). A total of 6846 Pacific oysters were identified and annotated, 3954 at the Scoble (Site A), and 2892 at the Collapit (Site B). Due to the overlapping nature of the images, many of those oysters were captured in different photos at different angles and light conditions.

Orthorectified tiles were then generated from the orthomosaic, as 640 × 640 pixel images for feeding into the Neural Network, which were tiled across the training and validation areas of each site.

This resulted in a dataset consisting of 3643 tiles for the Scoble site (758 containing Pacific oysters, 2885 without Pacific oysters) and 7571 tiles for the Collapit site (879 containing Pacific oysters and 6692 without Pacific oysters).

2.3. Validation and training datasets

To create the training and validation datasets, the tiles containing Pacific oysters were split into 70% training, and 30% validation. Data augmentation was used to increase the size of the training dataset, through random variations and manipulations to the data. Augmentations were applied in a random order. The list of augmentations is described in Table 1.

The training data set had five augmented images created per original tile to create an additional 5735 tiles split between the two sites. Augmentation was not applied to the validation data. An additional 300 tiles containing no Pacific oysters from each site were added to the training data set and 50 into the validation dataset to ensure that the model does not overestimate the number of Pacific oysters. This produced a training dataset of 7482 tiles, 3996 tiles for Scoble (Site A) and 3486 tiles for Collapit (Site B), and a validation dataset of 540 tiles, 288 tiles for Scoble (Site A) and 252 tiles for Collapit (Site B).

Table 1
Data Augmentations applied to training data.

Augmentation	Minimum	Maximum
Flip	–	–
Crop	0	10%
Contrast Shift	−25%	+50%
Translation	−20%	20%
Rotation	−90°	+90°

2.4. Deep learning models

Two widely used object detection models were selected for comparison, YOLOv5 (Jocher et al., 2021) and Faster R-CNN (FR-CNN) (Ren et al., 2015). YOLO is a lightweight approach where objects are identified directly through as single pass, whereas the FR-CNN is a multi-stage network approach based on identifying potential regions and then categorising and discarding some inappropriate regions (Ren et al., 2015). For the YOLOv5 model, we also tested three variants, YOLOv5 small, YOLOv5 medium and TPH-YOLOv5 (Zhu et al., 2021b), which is a modified variant of YOLO with a Transformer Prediction Head (TPH) (Yang et al., 2019).

The TPH-YOLOv5 model was pre-trained with the VisDrone dataset (Zhu et al., 2021a), and the YOLOv5m, YOLOv5s and FR-CNN models were pre-trained on the COCO dataset (Lin et al., 2014), to leverage the advantages of transfer learning (Safonova et al., 2023).

All models were trained to detect bounding boxes around Pacific oysters with a batch size of 16 image tiles, except for YOLOv5s, which needed to be trained with a batch size of 128, due to being a smaller model size. Models were all trained for 50 epochs (number of iterations over the training dataset in one cycle). Visual inspection of the training and validation loss curves showed that 50 epochs were sufficient for each model to reach convergence. As can be seen in Fig. 5, the loss plateau's then slowly rises for the object loss, thus no more training was required.

When taking the trained model for further inference, we selected the *best* model, based on the validation loss curve metrics, which means that the model selected was the one trained until epoch 6 (from the 50 epochs trained). The full loss curve is included for completeness.

Using the two independent validation dataset for each study site, result metrics were calculated using Padilla et al. (2021) for each DL model. A positive detection is identified where the Intersection over Union is greater than 0.5. As such, when detecting of a Pacific oyster, a detection overlaps with a true Pacific oyster by more than 50% of the bounding boxes. Consequently, we are able to classify each detection as one of the three categories:

True Positive (TP): A successfully detected Pacific oyster.

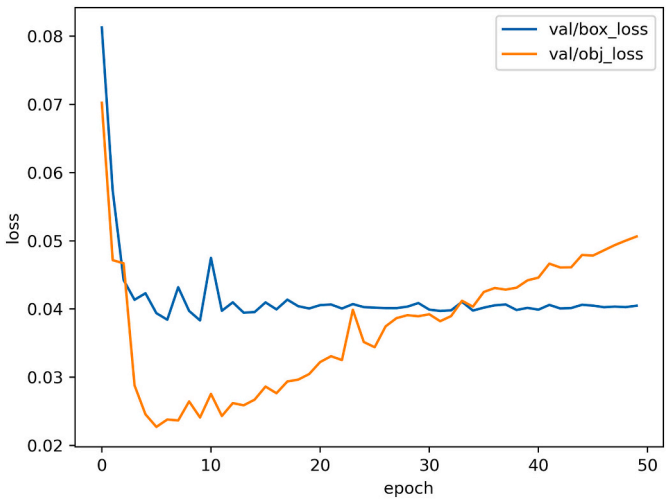

Fig. 5. Plot of the Validation Loss curve for the YOLOv5s model.

False Positive (FP): An incorrect detection, where no Pacific oyster exists, but one is predicted - such as a rock that has been misclassified.

False Negative (FN): Where a Pacific oyster is not detected.

The real number of Pacific oysters that were present in the field and were labelled within the validation dataset for each site is also referred as the **Ground Truth** and is used to obtain the metrics for each model. From this, we can calculate the precision and recall metrics, which was performed using Padilla et al. (2021).

$$\text{Precision} = \frac{TP}{TP + FP} = \frac{TP}{\text{Number Detected}}$$

$$\text{Recall} = \frac{TP}{TP + FN} = \frac{TP}{\text{Ground Truth}}$$

The uncertainties of precision and recall for each model are also estimated by calculating the Confidence Interval (CI) for each metric as:

$$\text{CI} = (Metric) \pm z \times SE_{metric}$$

where z is the z-score that corresponds to $z \approx 1.96$ for a 95% confidence assuming a normal distribution and the Standard Error (SE) defined as:

$$SE_{\text{Precision}} = \sqrt{\frac{\text{Precision} \times (1 - \text{Precision})}{\text{Number Detected}}}$$

and

$$SE_{\text{Recall}} = \sqrt{\frac{\text{Recall} \times (1 - \text{Recall})}{\text{Ground Truth}}}$$

Furthermore, in order to establish the balance between the precision and recall of each model, the F-score is also calculated as the harmonic mean of precision and recall uncertainty of the model:

$$\text{F-score} = 2 \times \frac{Precision \times Recall}{Precision + Recall}$$

3. Results

The results are presented in Table 2, which shows the evaluation scores for each model using the data from both sites combined as well as split into the two different evaluation sites with the different backgrounds of rocky shore and mudflats respectively. For each case, the models that return the higher number of true positives, the lower number of false negatives and those that score best on precision and recall, are highlighted in bold.

The results show YOLOv5s model performs best in both site, with precision scores of $\approx 88 - 89\%$. On the mudflats site, both YOLOv5s and TPH-YOLOv5 are almost exactly matched for precision scores (with a difference in precision below 0.05%) though YOLOv5s shows a higher recall (80% vs 68%). If the recall is prioritised over precision, then the FRCNN model performs best across all sites. For YOLO models, results indicate that some Pacific oysters are not being detected, however the models present higher confidence in those identifications as the number of false positives is much lower than FRCNN. As such, FRCNN is overestimating the number of Pacific oysters as it is detecting more than the Ground Truth number across both sites.

Similarly, the F-scores and Confident Intervals (CI) are shown on Table 3 to give an estimation of the uncertainties of each model and the balance between precision and recall. In all cases, YOLOv5s presents a higher F-score of approximately 85% which indicates a better trade-off between precision and recall than the other models. The 95% confident interval for precision is 86.7% - 89.7% meaning that the true precision of the YOLO5s model across both sites is 88.2% with a margin of error of 1.5%. In other words, we are 95% confident that 88.2% $\pm$ 1.5% of the detection raised by YOLO5s are indeed Pacific oyster. Similarly, the 95% confidence interval for YOLO5s recall is 80.7% - 84.1% which is equivalent to say that it might miss to identify between 15.9% - 19.3% of the Pacific oysters. FRCNN presents the second best F-score but it presents however the largest differences between precision and recall metrics sacrificing precision for higher recall values. As such, the FRCNN model is 95% confident that is detecting 90.2% of the Pacific oysters across both sites with an uncertainty of 0.4%. However, FRCNN's precision is 75.3% $\pm$ 1.8%, hence between 22.9% - 26.5% of the positives will not be Pacific oysters (likely rocks and other artifacts).

The prioritisation of precision or recall is an important distinction. In our case of study, we chose to reduce as much as possible the number of false negatives to increase the confidence and ensure the highest percentage of detected Pacific oysters are indeed Pacific oysters (and not rocks for example). This is particularly important when organising actions that might involve costly intervention schemes to manage the expansion of wild Pacific oysters at early stages. Hence, we determine that in this case the model that performs best is the one that favors precision over recall to ensure the Pacific oyster population is not overestimated: YOLOv5s. If we were targeting an approach where a larger number of false positives was acceptable to reduce as much as possible the number or false negatives or missed detection, then the recall metric would take precedence and FRCNN will be more appropriate even with a lower F-score.

To further explore the occurrence of false positives, we visualised some detection cases for the FRCNN, TPH-YOLO and YOLOv5s models. As shown in Fig. 6, there is a consistent under-performance in the detection across the mudflats region (Site A), particularly for the TPH model. In the rocky shore cases shown in Fig. 6, some rocks were incorrectly identified as Pacific oysters. Visual inspection of these figures can shed some light on why the models fail in different environments.

Lastly, the trained YOLO5s model was run over all tiles composing the entire data orthomosaic to create density maps of the surveyed regions. The orthomap and bounding boxes of the detected Pacific oysters

Table 2
Validation results from the four models, for each Site (A and B).

DL Model	Ground Truth	Number Detected	True Positives	False Negatives	False Positives	Precision	Recall
			Both Sites				
FRCNN	1829	2191	**1650**	**179**	541	0.753	**0.902**
TPH-YOLOv5	1829	1594	1257	572	337	0.789	0.687
YOLOv5s	1829	1709	1508	321	**201**	**0.882**	0.824
YOLOv5m	1829	1751	1446	383	305	0.826	0.791
			Collapit Mudflat (Site A)				
FRCNN	1025	1225	**916**	**109**	309	0.748	**0.894**
TPH-YOLOv5	1025	796	699	326	**97**	**0.878**	0.682
YOLOv5s	1025	935	821	204	114	**0.878**	0.801
YOLOv5m	1025	970	784	241	186	0.808	0.765
			Scoble Point Rocky Shore (Site B)				
FRCNN	804	966	**734**	**70**	232	0.760	**0.913**
TPH-YOLOv5	804	798	558	246	240	0.699	0.694
YOLOv5s	804	774	687	117	**87**	**0.888**	0.854
YOLOv5m	804	781	662	142	119	0.848	0.823

Table 3
F-scores, Standard Error and Confident Intervals for each model.

Model	F-score	Std Err Precision	CI_Precision Lower Limit	CI_Precision Upper Limit	Std Err Recall	CI_Recall Lower Limit	CI_Recall Upper Limit
				Both Sites			
FRCNN	0.821	0.009	0.735	0.771	0.007	0.888	0.916
TPH-YOLOv5	0.734	0.010	0.769	0.809	0.011	0.666	0.708
YOLOv5s	**0.852**	0.008	0.867	0.897	0.009	0.807	0.841
YOLOv5m	0.808	0.009	0.808	0.844	0.010	0.772	0.810
				Collapit Mudflat (Site A)			
FRCNN	0.814	0.012	0.724	0.772	0.010	0.874	0.912
TPH-YOLOv5	0.768	0.012	0.855	0.901	0.015	0.653	0.711
YOLOv5s	**0.838**	0.011	0.857	0.899	0.012	0.777	0.825
YOLOv5m	0.783	0.013	0.776	0.826	0.013	0.739	0.791
				Scoble Point Rocky Shore (Site B)			
FRCNN	0.830	0.014	0.733	0.787	0.010	0.894	0.932
TPH-YOLOv5	0.696	0.016	0.667	0.731	0.016	0.662	0.726
YOLOv5s	**0.871**	0.011	0.866	0.910	0.012	0.830	0.878
YOLOv5m	0.835	0.013	0.823	0.873	0.013	0.797	0.849

were transformed into the UTM (Universal Transverse Mercator) projection and the number of oysters per square meter was calculated using 1×1 m grid via the open source package QGIS. The result is a grid map that displays the density and location of the wild Pacific oysters spread in our study sites as shown on Figs. 7 and 8.

A total of 11,943 Pacific Oysters were detected at Collapit Creek and 2518 at Scoble Point. The density per square meter of Pacific oysters is larger at Collapit Creek as expected from previous reports (Natural England, 2021). These grid maps allow for easy visualization of the Pacific oysters density to locate hotspots and make possible regular monitoring to analyse trends.

A GitHub repository of the selected YOLO5s pretrained model has been made available, to provided a tutorial on how to apply the developed train model on new orthorectified images.[2]

4. Discussion

The expansion of wild Pacific oysters pose a threat to ecosystems of marine protected areas across Europe (Herbert et al., 2016; Natural England, 2021). Current models predict that their expansion will continue or accelerate due to warmer waters resulting from climate change (King et al., 2020; Rinde et al., 2017; Wilson et al., 2024). Hence, there is an urgent need to monitor their expansion to provide the pivotal information for early assessment and management action before their numbers can form reefs that might alter the balance of protected biomes (Natural England, 2021; Hansen et al., 2023; Reise et al., 2006). Moreover, monitoring the number of invasive wild Pacific oysters and their location is also vital to better understand the factors leading their spread, their impact, and to reduce the uncertainties of their expansion models (Wilson et al., 2024) as well as to provide the necessary data to promote regulations and ecological policies (Hansen et al., 2023).

This work presents a novel approach towards early detection and management of wild Pacific oysters expansion. We present a workflow for detecting, mapping and counting individual Pacific oysters using aerial drone imagery and DL.

Our approach identifies Pacific oysters using medium size object detection (50–300 pixels, Gong et al. (2022)). This method relies on morphological detection of juvenile or sexually mature Pacific oysters that have already acquired their distinctive colour and shape (that is different from their larvae) to be leveraged for their detection. Hence, by early detecting and mapping individual Pacific oysters, their expansion can be quantified, their hotpots assessed and remedial action can be planned before putting at risk marine protected areas (Reise et al., 2006).

The detection of Pacific oysters as medium size objects is fundamental to this study and allows the workflow proposed to become a successful monitoring solution that can be easily deployed on the field. While other researchers (Lin et al., 2022; Sadrfaridpour et al., 2021) have showed success in detecting individual Pacific oysters using CNN and segmentation or similarly, to detect morphological and colouring traits of cockle shells to identify their harvest locations (Concepcion et al., 2023), these studies are based on capturing individuals with the resolution needed to perform big object detection ($>$ 300 pixels). These methods require images with extremely high resolution and, in all cases, the distances between the camera and the Pacific oysters required are lower than a meter distance (reportedly 92–30 cm) to achieve pixel sizes of 0.06 or better and capture the oysters and cockles as objects with more than 300 pixels. This restriction on the distance between camera and target imposed by the resolution of big object detection means that these techniques are not feasible to be implemented to survey medium size areas ($\approx$1Ha) or larger due to the amount of hours that will demand for data collection (either using aerial or underwater drones or manually). On the other hand, Ridge et al. (2020) showed how CNN can be applied to aerial images collected at the altitudes of 100 m with a reported pixel size of 2.2 cm to delineate oyster reefs but not providing enough resolution to perform object detection and identify individual Pacific oysters. Therefore, selecting an appropriate pixel size for capturing Pacific oysters as medium size objects is key for ecological management for early detection and it is dictated by the camera parameters (focal length and number of pixels) and flight altitude (Andriolo et al., 2023). The pixel size can be easily calculated and adjusted when drafting a drone survey by entering the camera model or camera parameters and the flight altitude in any of the most common drone planning software tools including DJI GS PRO, Pix4D or Litchi.

While the data acquired in this work were collected at 0.3 cm/px (using a DJI Phantom4 Pro v2.0 at 10 m altitude), a lower resolution can be selected to fly at higher altitudes making possible to cover larger areas in the same span of time. In those cases, a pixel size or Ground Sampling Distance (GSD) better than 0.8 cm/px is required when planning the drone survey to capture common sizes of Pacific oysters within 50 pixels (usually around 8 cm long and 5 cm wide). Moreover, we recommend a resolution of 0.5 cm/px (cm per pixel) to be able to correctly detect Pacific oysters that might be partially covered by mud or algae. Using a resolution of 0.5 cm/px, the smallest Pacific oyster that can be detected within 50 pixels is 5 cm long and 3 cm wide (juvenile stage). This can be achieved with widely available consumer drones such as the DJI Phantom 4 (GSD of 0.5 cm at 18 m altitude). Using survey grade cameras with better shutter speed and pixel resolution such as the 35 mm lens DJI Zenmuse P1, the same resolution of 0.5 cm can be achieved at 40 m altitude, further increasing the area that can be covered on each drone campaign (approximately up to 15 Ha within 30 min).

This study compares different CNN models to detect Pacific oysters

[2] https://github.com/djmoffat/PacificOysterDetection

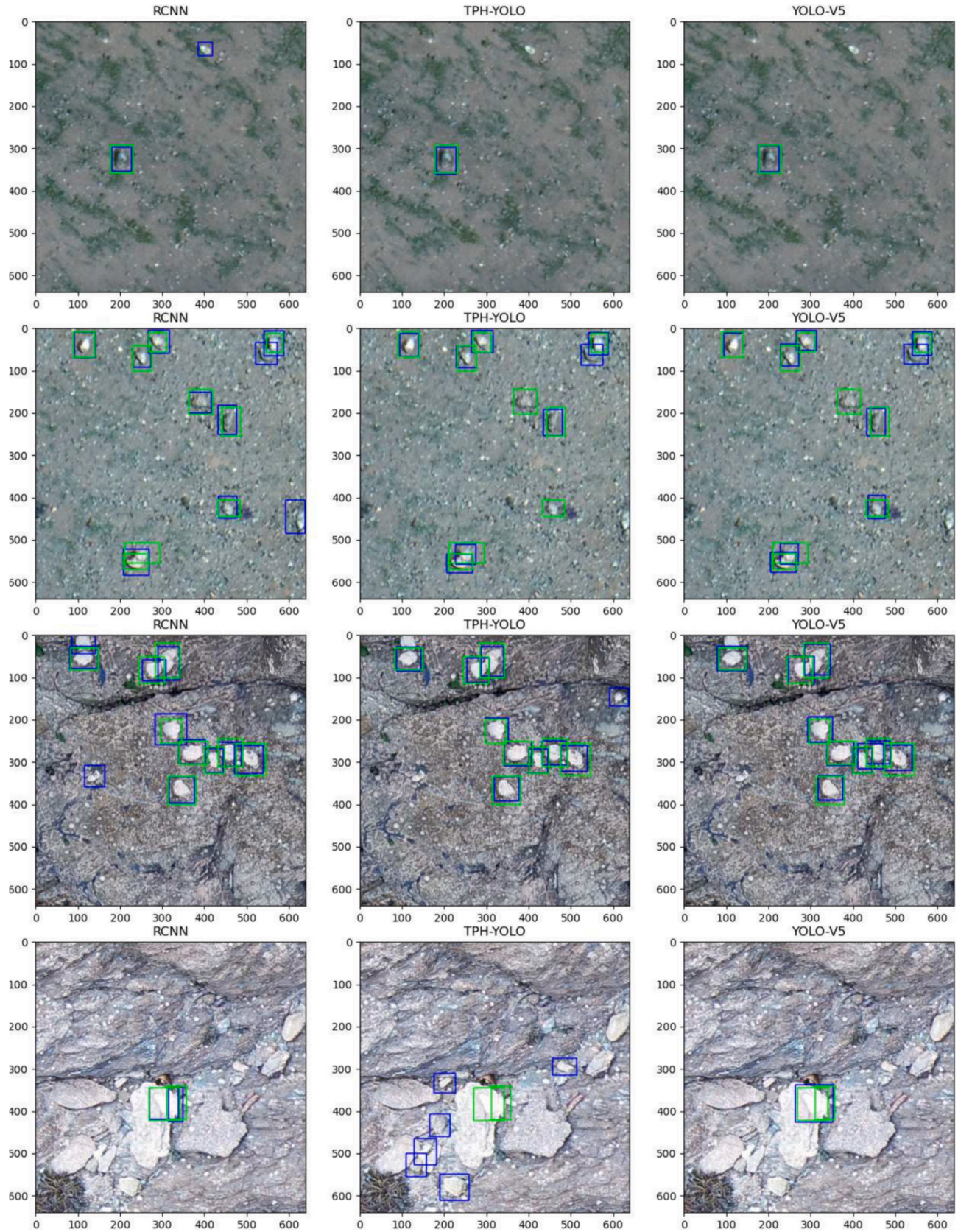

Fig. 6. Examples of four scenes with different method ML method comparison (FR-CNN, TPH-YOLOv5 and YOLOv5s) for detection across Site A - mudflats (first and second rows of images) and Site B - rocky shoreline (third and fourth rows). Green boxes are the Ground Truth data and blue boxes are the detected Pacific oysters for each model. Hence, boxes colored by green and blue indicate true positive, and boxes colored by only green or only blue indicate respectively a false negative and false positive. (For interpretation of the references to colour in this figure legend, the reader is referred to the web version of this article.)

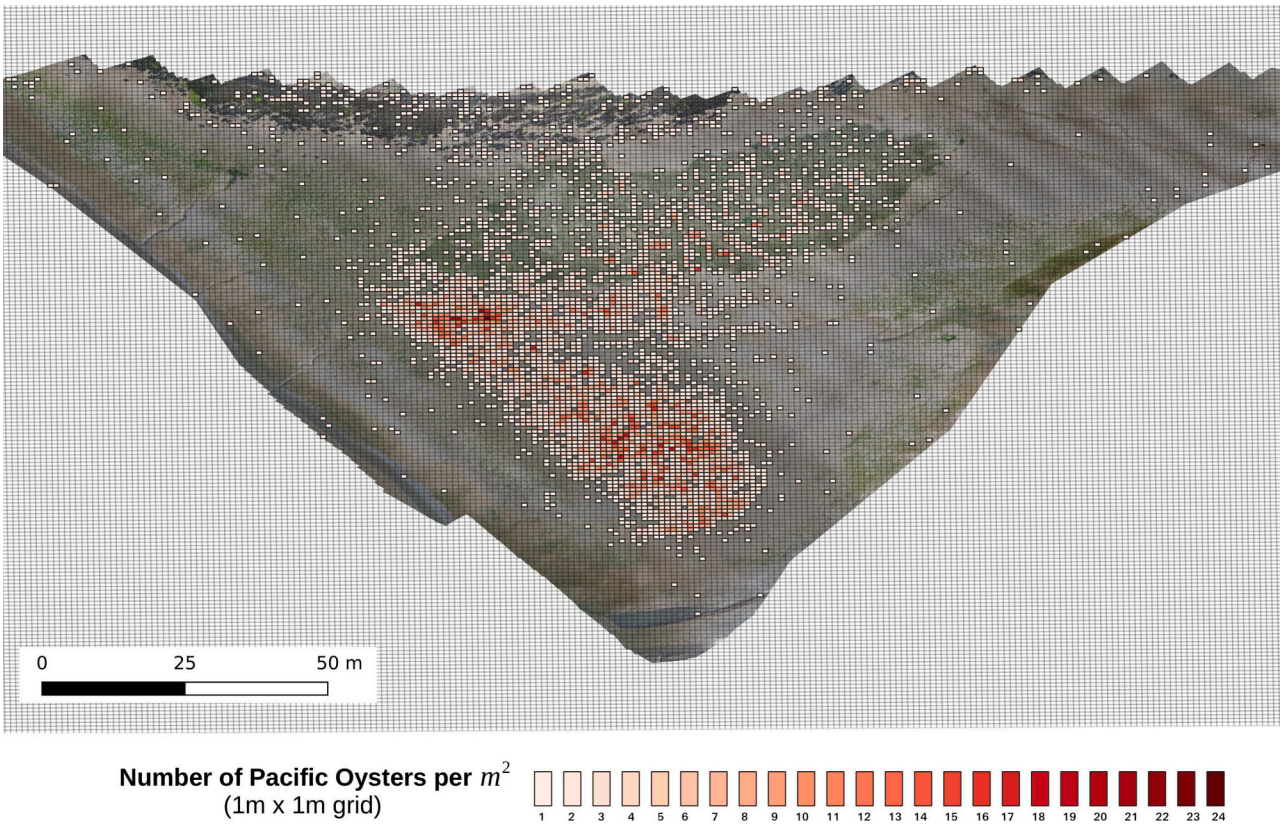

Fig. 7. Pacific Oyster population per square meter over the mudflat area surveyed at Collapit Creek (Site A). A total of 11,943 Pacific Oysters were detected.

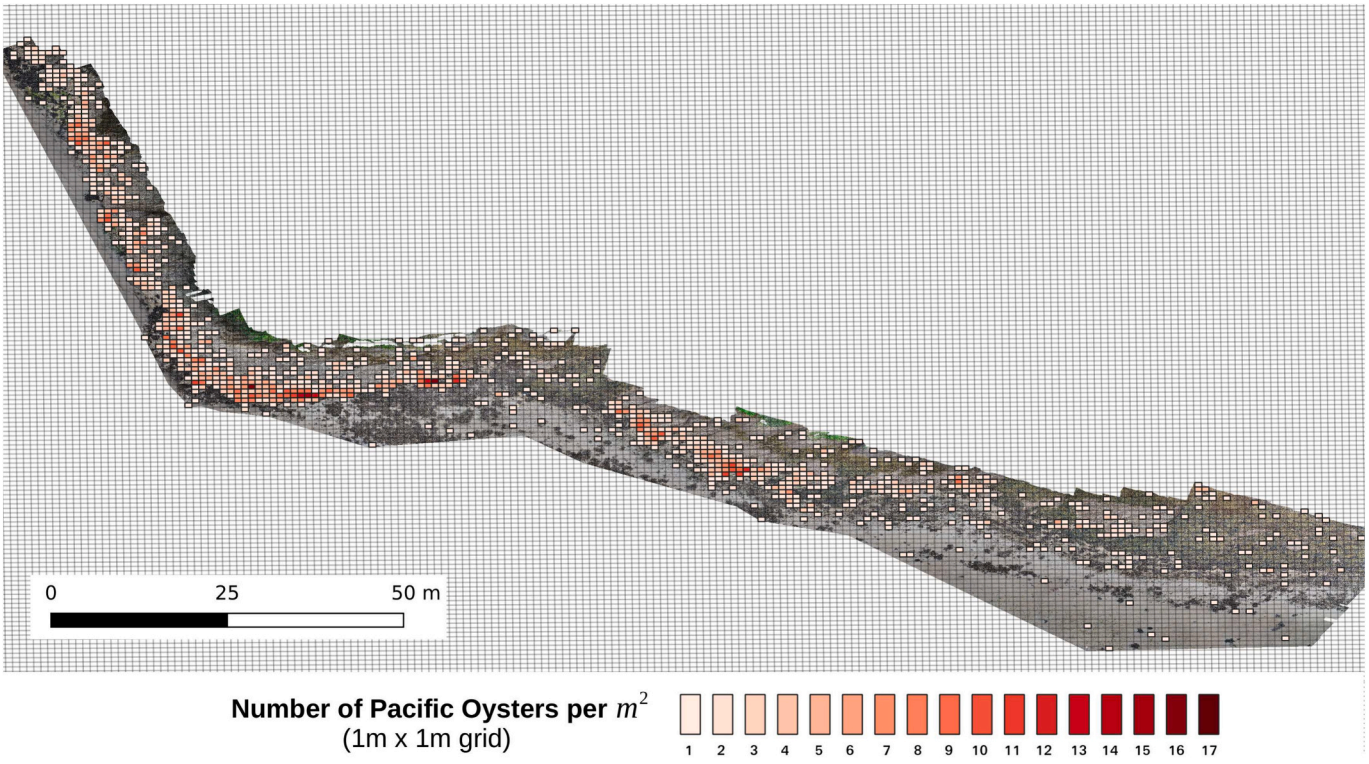

Fig. 8. Pacific Oyster population per square meter over the rocky shore at Scoble Point (Site B). A total of 2518 Pacific Oysters were detected.

and reports a model precision up to 88% both for the intertidal areas of rocky shores and mudflats. We apply our trained YOLOv5s model to two distinctive cases at Kingsbridge Estuary (UK) and present an estimation of their population in a grid map. This allows for easy visualization and the creation of time series to investigate trends or seasonal effects.

A comprehensive cost analysis for drone surveys versus traditional surveys has been produced by White et al. (2022). Correspondingly, aerial drone surveys can provide cost-effective solutions to monitor Pacific oysters in contrast to compared to traditional walk-over surveys which typically rely on volunteers. Another advantage of the workflow presented in this publication versus traditional surveys is that each Pacific oyster is visible and geolocated in the orthomap. This contributes to identifying hotpots and areas at risk as well as enables the creation of time series by collecting data over the same region. This grants a more efficient solution than using manual methods which typically will require manually recording the GPS location for each oyster to be logged. The inclusion of UTM grid density maps enhances data assimilation delivering powerful visualization tools of the DL model outputs to easily assess the Pacific oyster population per square meter in the surveyed terrain (Figs. 7 and 8). Additionally, the use of RPAS can provide the necessary data from areas that are not easy or safe to access (Jaud et al., 2019) such as the Collapit Creek mudflats surveyed in this work.

Several DL architectures were compared for their effectiveness in the detection Pacific oysters. YOLOv5s presented the best model precision while the best recall was FRCNN. This indicates that YOLOv5s is the most appropriate model for use in this domain, due to the precision being significantly higher than FRCNN (88% for YOLOv5s and YOLOv5m vs 75% for FRCNN) while the recall of both models is closer (82% for YOLOv5s vs 79% YOLOv5m). Prioritising precision over recall means that we minimise the number of false positives (the number of objects incorrectly raised as Pacific oysters), therefore the model is more likely to correctly detect Pacific oysters but it might underestimate their population. The YOLOv5s model has been trained to detect individual oysters at the different landscapes of mudflat and rocky shores with an precision of 88% and a marginal difference below 0.5% between the two sites and with a 95% confidence accuracy of 1.5%. Similarly, YOLO5s presents a recall of 80.7% - 84.1% with a 95% confidence. These values ensure that the model is practical and can be implemented for ecological management but caution should be exercised when comparing this precision to other published work that relies on big object detection instead of medium size detection used in this paper. As such Sadrfaridpour et al. (2021) reports a similar average precision of 81.8% when detecting submerged Pacific oysters within 3 ft of distance (0.92 cm, big object detection). While Concepcion et al. (2023) reports precision of their model to detect common cockle harvest origin using CNN up to 96% using photos taken at 50 cm distance. To the best of knowledge of the authors, no study has been published that uses medium size detection to identify oysters or moluscs and reports the precision of the model.

As three of our models are based on the YOLO structure, we would expect the results to be relatively similar, and the results demonstrate the success on small training data quantities compared to larger model complexity. Intuitively, it would be expected that a smaller model can successfully learn from fewer data to represent less complex problems, whereas larger more complex models may require more data to represent more complexity within the object to detect. The results indicated that YOLOv5s, as the smallest model, performs best in terms of precision. The TPH-YOLOv5, which is an extension of the YOLOv5s model is a slightly more complex model, and further pre-training on RPAS specific imagery. The results indicated that detection of Pacific oysters does not demand the complexity of the larger YOLOv5m model and using the TPH-YOLOv5 model pre-trained with RPAS data, is not beneficial in this instance.

As shown on Fig. 6, the trained YOLOv5s model was able to detect Pacific oysters against the different backgrounds of mud, vegetation, different rocks and both when the oysters were found as individuals far away from each other or growing together in close proximity in large numbers. This is representative of a large number of environments across Europe. Hence, the workflow presented is transferable to those areas and our CNN model should be able to generalize to new sites. However, more data are required to validate this claim. Furthermore, due to the constrains of this project, only a limited number of oysters could be tagged as a training and validation dataset and the model would benefit from including more data over different backgrounds to be further fine-tuned.

The authors recognize several other limitations that could be addressed in follow up projects. First, only two types of neural network architectures were used, whereas additional benchmarking could be performed with other types of ResNets, DenseNets and transformer based models. Secondly, this study does not address the individual insights from the trained models, and the pros and cons of architectures and hyperparameters in recognizing specific features of Pacific oysters across mudflats and rocky shore imagery. Thirdly, ablations studies should be performed, showcasing the possibilities for reducing the complexities of neural network layers and speeding up the computation times. And fourthly, if left unmanaged, Pacific oysters can create oyster reefs and very dense clusters where younger oysters grow on top of the older. In such cases, no gaps are found in the cluster and only the oysters on the top are partially visible (as shown on Fig. 1b). The equivalent density for those maximal density clusters are impossible to calculate using visual methods only and is sometimes estimated as over 200 oysters per square meter (Herbert et al., 2016). We expect that our current model will struggle to identify these large clusters and will not provide an appropriate population estimations in such cases. One potential approach to solve this issue would be to frame the task as object segmentation (Ridge et al., 2020). However, our study is designed for repeated and early detection on Pacific oysters before those clusters are established. Using this methodology, we argue that regular surveys can be undertaken over the same area to detect trends of growth and organise preventive measurements as needed in marine protected areas when it is still possible to manage the negative impact of Pacific oyster reefs (Hansen et al., 2023).

This work has been carried out on very different regions that are representative of many different environments across Europe. We also performed data augmentation on the training the model including varying lighting conditions that ensure it represents seasonal or daily variations in the conditions. Thus, the model has the potential to be expanded and validated to other areas across Europe where the spread of wild Pacific oysters can pose a challenge. While this work has focused on the detection at early stages of colonisation to preserve marine protected areas, the CNN model could also be expanded to estimate the densities of large Pacific oyster reefs that include clusters with over 200 oysters per square meter presenting little to none substrate visible. In a similar manner, the model could also be further developed to include the separate detection of other species of molluscs due to their morphological differences that might compete in the same environment, so long as those molluscs can be detected within the intertidal zone using medium size object detection.

5. Conclusions

This study presents the results and workflow of mapping emerged wild Pacific oysters using low altitude RPAS imagery to estimate and visualize their density for ecological management purposes. These data are essential to better understand the impact of Pacific oysters, establish regulation policies and to early detect the colonisation of marine protected sites that put these ecosystems at risk. We compared how different CNNs models including YOLOv5s, YOLOv5m, TPH-YOLOv5 and FR-CNN performed medium object detection to identify Pacific oysters both on intertidal rocky shores and mudflat regions. We report metrics of each model with precision scores up to 88% with only a marginal 1% difference across the different sites. The workflow proposed includes how the output of the model can be visualised on an UTM projected grid

map to efficiently assess the number of Pacific oysters per square meter for management purposes which level of detail is not possible or extremely laborious to achieve using traditional surveys. The use of drones and DL therefore provides a cost-effective monitoring solution while can also provide data over complex terrain that in many cases is otherwise unreachable via "walk-over" surveys.

Funding

AM, **DM**, **WJ**, **KAC**, **VB**, **SG** were supported by the PORTWIMS Project, European Union's Horizon 2020 research and innovation program under grant agreement No 810139. **SA** was supported by a doctoral fellowship by the FCT (UI/BD/151020/2021). **MR** was supported by the FCT project INTERWHALE - Advancing Interactive Technology for Responsible Whale-Watching, with grant No PTDC/CCI-COM/0450/2020. **OT** was supported by Marine Research Plymouth as part of his PhD. **NM** was supported by South Devon AONB Estuaries Partnership.

CRediT authorship contribution statement

Aser Mata: Conceptualization, Methodology, Investigation, Writing – original draft, Writing – review & editing, Visualization, Supervision. **David Moffat:** Formal analysis, Software, Writing – review & editing, Validation. **Sílvia Almeida:** Funding acquisition, Resources, Writing – review & editing. **Marko Radeta:** Writing – review & editing. **William Jay:** Data curation, Resources. **Nigel Mortimer:** Funding acquisition, Resources, Writing – review & editing. **Katie Awty-Carroll:** Software. **Oliver R. Thomas:** Funding acquisition. **Vanda Brotas:** Funding acquisition. **Steve Groom:** Project administration, Funding acquisition.

Declaration of competing interest

The authors declare that they have no conflicts of interest.

Data availability

Data will be made available on request.

Acknowledgements

The authors thank the NERC Earth Observation Data Acquisition and Analysis Service (NEODAAS) for access to computing facilities for developing and training the DL models. Special thanks to Nigel Mortimer for organising and providing support in the field campaign.

References

Andriolo, U., Gonçalves, G., Bessa, F., Sobral, P., 2020. Mapping marine litter on coastal dunes with unmanned aerial systems: a showcase on the Atlantic coast. Sci. Total Environ. 736, 139632 https://doi.org/10.1016/j.scitotenv.2020.139632.

Andriolo, U., Garcia-Garin, O., Vighi, M., Borrell, A., Gonçalves, G., 2022. Beached and floating litter surveys by unmanned aerial vehicles: operational analogies and differences. Remote Sens. 14 https://doi.org/10.3390/rs14061336.

Andriolo, U., Topouzelis, K., van Emmerik, T.H., Papakonstantinou, A., Monteiro, J.G., Isobe, A., Hidaka, M., Kako, S., Kataoka, T., Gonçalves, G., 2023. Drones for litter monitoring on coasts and rivers: suitable flight altitude and image resolution. Mar. Pollut. Bull. 195, 115521 https://doi.org/10.1016/j.marpolbul.2023.115521.

Concepcion, R., Guillermo, M., Tanner, S.E., Fonseca, V., Duarte, B., 2023. Bivalvenet: a hybrid deep neural network for common cockle (cerastoderma edule) geographical traceability based on shell image analysis. Eco. Inform. 78, 102344 https://doi.org/10.1016/j.ecoinf.2023.102344.

Diederich, S., 2006. High survival and growth rates of introduced Pacific oysters may cause restrictions on habitat use by native mussels in the Wadden Sea. J. Exp. Mar. Biol. Ecol. 328, 211–227. https://doi.org/10.1016/j.jembe.2005.07.012.

Gonçalves, G., Andriolo, U., Gonçalves, L.M., Sobral, P., Bessa, F., 2022. Beach litter survey by drones: mini-review and discussion of a potential standardization. Environ. Pollut. 315, 120370 https://doi.org/10.1016/j.envpol.2022.120370.

Gong, H., Mu, T., Li, Q., Dai, H., Li, C., He, Z., Wang, W., Han, F., Tuniyazi, A., Li, H., Lang, X., Li, Z., Wang, B., 2022. Swin-transformer-enabled yolov5 with attention mechanism for small object detection on satellite images. Remote Sens. 14 https://doi.org/10.3390/rs14122861.

Green, D.S., Crowe, T.P., 2014. Context-and density-dependent effects of introduced oysters on biodiversity. Biol. Invasions 16, 1145–1163. https://doi.org/10.1007/s10530-013-0569-x.

Hansen, B.W., Dolmer, P., Vismann, B., 2023. Too late for regulatory management on pacific oysters in european coastal waters? J. Sea Res. 191, 102331 https://doi.org/10.1016/j.seares.2022.102331.

Herbert, R., Roberts, C., Humphreys, J., Fletcher, S., 2012. The Pacific oyster (*Crassostrea gigas*) in the UK: economic, legal and environmental issues associated with its cultivation, wild establishment and exploitation. Rep. Shellfish Assoc. Great Britain 12012, 66.

Herbert, R.J.H., Humphreys, J., Davies, C.J., Roberts, C., Fletcher, S., Crowe, T.P., 2016. Ecological impacts of non-native Pacific oysters (*Crassostrea gigas*) and management measures for protected areas in Europe. Biodivers. Conserv. 25, 2835–2865. https://doi.org/10.1007/s10531-016-1209-4.

Jaud, M., Letortu, P., Théry, C., Grandjean, P., Costa, S., Maquaire, O., Davidson, R., Le Dantec, N., 2019. UAV survey of a coastal cliff face – selection of the best imaging angle. Measurement 139, 10–20. https://doi.org/10.1016/j.measurement.2019.02.024.

Jocher, G., Stoken, A., Borovec, J., Chaurasia, A., Changyu, L., Hogan, A., Hajek, J., Diaconu, L., Kwon, Y., Defretin, Y., et al., 2021. Ultralytics/yolov5: v5. In: 0-YOLOv5-P6 1280 Models, AWS, Supervisely and YouTube Integrations. Zenodo.

Kakehi, S., Sekiuchi, T., Ito, H., Ueno, S., Takeuchi, Y., Suzuki, K., Togawa, M., 2021. Identification and counting of Pacific oyster *Crassostrea gigas* larvae by object detection using deep learning. Aquac. Eng. 95, 102197 https://doi.org/10.1016/j.aquaeng.2021.102197.

King, N.G., Wilmes, S.B., Smyth, D., Tinker, J., Robins, P.E., Thorpe, J., Jones, L., Malham, S.K., 2020. Climate change accelerates range expansion of the invasive non-native species, the Pacific oyster, *Crassostrea gigas*. ICES J. Mar. Sci. 78, 70–81. https://doi.org/10.1093/icesjms/fsaa189.

Lin, T.Y., Maire, M., Belongie, S., Hays, J., Perona, P., Ramanan, D., Dollár, P., Zitnick, C. L., 2014. Microsoft coco: common objects in context. In: Computer Vision–ECCV 2014: 13th European Conference, Zurich, Switzerland, September 6-12, 2014, Proceedings, Part V 13. Springer, pp. 740–755.

Lin, X., Sanket, N.J., Karapetyan, N., Aloimonos, Y., 2022. Oysternet: Enhanced Oyster Detection using Simulation. preprint arXiv:2209.08176. https://doi.org/10.48550/arXiv.1506.01497.

Mata, A., 2024. Drone Orthomosaics for Remote Detection of Pacific Oysters (Kingsbridge Estuary, UK). Dataset. https://doi.org/10.5281/zenodo.11199071.

Natural England, 2021. Partnership Led Strategy to Monitor and Manage the Spread of Pacific Oyster Populations in South Devon and Cornwall - NERR100.

Padilla, R., Passos, W.L., Dias, T.L.B., Netto, S.L., da Silva, E.A.B., 2021. A comparative analysis of object detection metrics with a companion open-source toolkit. Electronics 10. https://doi.org/10.3390/electronics10030279.

Perry, F., Jackson, A., Garrard, S., Williams, E., Tyler-Walters, H., 2023. *Ostrea edulis* native oyster. In: Tyler-Walters, H. (Ed.), Marine Life Information Network: Biology and Sensitivity Key Information Reviews, [on-Line]. Marine Biological Association of the United Kingdom, Plymouth.

Radeta, M., Zuniga, A., Motlagh, N.H., Liyanage, M., Freitas, R., Youssef, M., Tarkoma, S., Flores, H., Nurmi, P., 2022. Deep learning and the oceans. Computer 55, 39–50. https://doi.org/10.1109/MC.2022.3143087.

Reise, K., Olenin, S., Thieltges, D.W., 2006. Are aliens threatening european aquatic coastal ecosystems? Helgol. Mar. Res. 60, 77–83.

Ren, S., He, K., Girshick, R., Sun, J., 2015. Faster R-CNN: towards real-time object detection with region proposal networks. Adv. Neural Inf. Proces. Syst. 28 https://doi.org/10.48550/arXiv.1506.01497.

Ridge, J.T., Gray, P.C., Windle, A.E., Johnston, D.W., 2020. Deep learning for coastal resource conservation: automating detection of shellfish reefs. Remote Sens. Ecol. Conserv. 6, 431–440. https://doi.org/10.1002/rse2.134.

Rinde, E., Tjomsland, T., Hjermann, D.Ø., Kempa, M., Norling, P., Kolluru, V.S., 2017. Increased spreading potential of the invasive Pacific oyster (*Crassostrea gigas*) at its northern distribution limit in Europe due to warmer climate. Mar. Freshw. Res. 68, 252. https://doi.org/10.1071/MF15071.

Ruesink, J.L., Lenihan, H.S., Trimble, A.C., Heiman, K.W., Micheli, F., Byers, J.E., Kay, M. C., 2005. Introduction of non-native oysters: ecosystem effects and restoration implications. Annu. Rev. Ecol. Evol. Syst. 36, 643–689. https://doi.org/10.1146/annurev.ecolsys.36.102003.152638.

Sadrfaridpour, B., Aloimonos, Y., Yu, M., Tao, Y., Webster, D., 2021. Detecting and counting oysters. In: 2021 IEEE International Conference on Robotics and Automation (ICRA). IEEE, pp. 2156–2162. https://doi.org/10.48550/arXiv.2105.09758.

Safonova, A., Ghazaryan, G., Stiller, S., Main-Knorn, M., Nendel, C., Ryo, M., 2023. Ten deep learning techniques to address small data problems with remote sensing. Int. J. Appl. Earth Obs. Geoinf. 125, 103569 https://doi.org/10.31223/X52H3B.

Schneider-Zapp, K., Cubero-Castan, M., Shi, D., Strecha, C., 2019. A new method to determine multi-angular reflectance factor from lightweight multispectral cameras with sky sensor in a target-less workflow applicable to UAV. Remote Sens. Environ. 229, 60–68. https://doi.org/10.48550/arXiv.1905.03301.

Takaya, K., Shibata, A., Mizuno, Y., Ise, T., 2022. Unmanned aerial vehicles and deep learning for assessment of anthropogenic marine debris on beaches on an island in a semi-enclosed sea in Japan. Environ. Res. Commun. 4, 015003 https://doi.org/10.1088/2515-7620/ac473b.

Tzutalin, D., 2015. LabelImg. Github. URL. https://github.com/HumanSignal/labelImg.

Utting, S., Spencer, B., 1992. Introductions of marine bivalve molluscs into the united kingdom for commercial culture–case histories. In: Marine Science Symposia. International Council for the Exploration of the Sea, Copenhagen, pp. 84–91.
Walne, P., Helm, M., 1979. Introduction of crassostrea gigas into the United Kingdom. In: Exotic Species in Mariculture. MIT Press, Cambridge, Mass, pp. 83–105.
White, S.M., Schaefer, M., Barfield, P., Cantrell, R., Watson, G.J., 2022. Cost benefit analysis of survey methods for assessing intertidal sediment disturbance: a bait collection case study. J. Environ. Manag. 306, 114386 https://doi.org/10.1016/j.jenvman.2021.114386.
Wierzbicki, D., 2018. Multi-camera imaging system for UAV photogrammetry. Sensors 18, 2433. https://doi.org/10.3390/s18082433.
Wilson, R.J., Kay, S., Ciavatta, S., 2024. Partitioning climate uncertainty in ecological projections: Pacific oysters in a hotter europe. Eco. Inform. 102537. https://doi.org/10.1016/j.ecoinf.2024.102537.
Yang, F., Fan, H., Chu, P., Blasch, E., Ling, H., 2019. Clustered object detection in aerial images. In: Proceedings of the IEEE/CVF International Conference on Computer Vision, pp. 8311–8320. https://doi.org/10.48550/arXiv.1904.08008.
Zhu, P., Wen, L., Du, D., Bian, X., Fan, H., Hu, Q., Ling, H., 2021a. Detection and tracking meet drones challenge. IEEE Trans. Pattern Anal. Mach. Intell. 44, 7380–7399. https://doi.org/10.1109/tpami.2021.3119563.
Zhu, X., Lyu, S., Wang, X., Zhao, Q., 2021b. TPH-YOLOv5: improved yolov5 based on transformer prediction head for object detection on drone-captured scenarios. In: Proceedings of the IEEE/CVF International Conference on Computer Vision, pp. 2778–2788. https://doi.org/10.48550/arXiv.2108.11539.